AIAA 80-1643R

Time-Optimal Magnetic Attitude Maneuvers

J.L. Junkins* and C.K. Carrington†
Virginia Polytechnic Institute and State University, Blacksburg, Va.
C.E. Williams‡
The Johns Hopkins Applied Physics Laboratory, Laurel, Md.

Time-optimal magnetic attitude maneuvers for near-Earth spin-stabilized spacecraft are treated using Pontryagin's Principle. A nonlinear bang-bang switching function is derived for the electromagnets' polarity. The approach is quite general, allowing user-prescribed orbit dynamics models and geomagnetic field models. For the case of a single electromagnet aligned with the nominal spin axis of a symmetric satellite, and retaining general orbit and geomagnetic models, the determination of time-optimal magnetic maneuvers reduces to a bounded one-dimensional search of an initial costate variable. The formulation is used to construct extremal field maps of typical optimal maneuvers and is further used to determine "for example" time-optimal maneuvers for the NOVA navigational satellite scheduled for launch in the spring of 1981.

Introduction

SEVERAL investigators[1-12] have developed and applied control laws for generating magnetic torques for 1) precession/nutation damping, 2) momentum dumping (from reaction wheels), and 3) large-angle maneuvers. Spacecraft that are presently operational utilize (or have utilized) all three types of magnetic torque strategies. Apparently none of the large-angle maneuvers of existing spacecraft have been of the minimum time variety, although typical large-angle maneuvers require hours or even days to complete. Perhaps the anticipation of a complicated nonlinear two-point boundary-value problem (TPBVP) has deterred effort in this direction.

Tossman[1] formulated time-optimal magnetic control necessary conditions under the assumption that the Earth's magnetic field was a nonrotating dipole. Tossman also artificially introduced an approximate form for a switching function, which made the already qualitative nature of his developments of questionable utility. Tossman's work, however, led to an elegantly simple one-dimensional TPBVP approximate optimal maneuver.

The present paper was motivated by the work of Tossman,[1] but we decided at the onset to retain the generality of using state-of-the-art orbit integrators and magnetic field models. As is shown below, we developed a time-optimal "slow maneuver formulation" which retains the most attractive feature of a bounded one-dimensional search to solve the resulting two-point boundary-value problem.

Kinematics and Dynamics

Consider the angular motion of a spin-stabilized symmetric spacecraft (Fig. 1). A despun, dextral coordinate frame $\{\hat{d}\}$ is associated with the vehicle such that $\hat{d}_3$ is along the axis of symmetry (right ascension α, declination δ) and $\hat{d}_1$ lies in the inertial $(\hat{n}_1,\hat{n}_2)$ plane as shown.

The spacecraft (S) angular velocity is then

$$\omega_S = \dot{\alpha}\hat{n}_3 - \dot{\delta}\hat{d}_1 + \dot{\phi}\hat{d}_3 \tag{1}$$

where $\dot{\phi}$ is the vehicle spin velocity relative to the $\{\hat{d}\}$ frame, and $(\dot{}) \equiv \mathrm{d}/\mathrm{d}t(\ )$.

The angular velocity of the despun frame (D) is clearly

$$\omega_D = \omega_S - \dot{\phi}\hat{d}_3 = \dot{\alpha}\hat{n}_3 - \dot{\delta}\hat{d}_1 \tag{2}$$

For subsequent use, orthogonal components of ω_S and ω_D are taken along the $\{\hat{d}\}$ basis vectors as

$$\omega_S = \omega_1\hat{d}_1 + \omega_2\hat{d}_2 + \omega_3\hat{d}_3 \qquad \omega_D = \Omega_1\hat{d}_1 + \Omega_2\hat{d}_2 + \Omega_3\hat{d}_3 \tag{3}$$

where

$$\omega_1 = \Omega_1 = -\dot{\delta} \qquad \omega_2 = \Omega_2 = \dot{\alpha}\cos\delta \qquad \omega_3 = \Omega_3 + \dot{\phi}$$

and

$$\Omega_3 = \dot{\alpha}\sin\delta$$

The equations of motion follow from

$$\text{torque} = {}^N\mathrm{d}/\mathrm{d}t(\text{angular momentum}) \tag{4a}$$

or with $\{\hat{d}\}$ components

$$\sum_{i=1}^{3} T_i\hat{d}_i = \frac{{}^D\mathrm{d}}{\mathrm{d}t}\left(\sum_{i=1}^{3} I_i\omega_i\hat{d}_i\right) + \left(\sum_{j=1}^{3}\Omega_j\hat{d}_j\right)\times\left(\sum_{i=1}^{3} I_i\omega_i\hat{d}_i\right) \tag{4b}$$

where ${}^D\mathrm{d}/\mathrm{d}t\ (\ )$ is the time derivative of $(\ )$ as seen from frame R, $A(\equiv I_1 = I_2)$ is the transverse centroidal moment of inertia, and $C(\equiv I_3)$ is the spin axis centroidal moment of inertia. Carrying out the algebra implied in Eqs. (4) and equating components yields the scalar equations of motion

$$\begin{aligned} T_1 &= -A\ddot{\delta} + (C-A)\,\dot{\alpha}^2\sin\delta\cos\delta + (C\dot{\phi})\,\dot{\alpha}\cos\delta \\ T_2 &= A\ddot{\alpha}\cos\delta + C\dot{\alpha}\dot{\delta}\sin\delta + (C\dot{\phi})\,\dot{\delta} - 2A\dot{\alpha}\dot{\delta}\sin\delta \\ T_3 &= C\ddot{\alpha}\sin\delta + C\dot{\alpha}\dot{\delta}\cos\delta + C\ddot{\phi} \end{aligned} \tag{5}$$

For spin-stabilized satellites, the spin momentum terms (multiplied by $H_3 \equiv C\dot{\phi}$) generally dominate Eqs. (5). Under the "slow maneuver" assumption, one can often approximate the right side of Eqs. (5) by

$$T_1 \cong H_3\dot{\alpha}\cos\delta \qquad T_2 \cong H_3\dot{\delta} \qquad T_3 \cong \dot{H}_3 \tag{6}$$

Received May 28, 1980; presented as Paper 80-1643 at the AIAA/AAS Astrodynamics Conference, Danvers, Mass., Aug. 11-13, 1980; revision received Oct. 9, 1980.

*Professor of Engineering Science and Mechanics; Consultant to The Johns Hopkins Applied Physics Laboratory. Associate Fellow AIAA.

†Member of the Technical Staff, Space Development Department.

‡Research Associate, Ph.D. candidate.

from which we obtain the widely used approximate rates for slewing of the spin axis

$$\dot{\alpha} \cong T_1/H_3 \cos\delta \qquad \dot{\delta} \cong T_2/H_3 \tag{7}$$

Equations (7) can also be derived by assuming that the symmetry axis always remains aligned with the instantaneous angular momentum vector, so an alternate interpretation of the slow maneuver assumption is that the coning motion about the angular momentum vector is always of small amplitude. As is well-known, solutions based upon integrating $(\alpha,\delta,\phi,\dot{\alpha},\dot{\delta},\dot{\phi})$ from Eqs. (5) typically oscillate with small amplitude (for well-damped, spin-stabilized satellites) about the (α,δ) solution based upon Eqs. (7).

The magnetic torque vector is given by

$$\boldsymbol{T} = \boldsymbol{M} \times \boldsymbol{\beta} \tag{8}$$

where

$$\boldsymbol{M} = pM\hat{d}_3 \tag{9}$$

is the spacecraft dipole moment with constant magnitude M and polarity $p\,(-1,0,1)$,

$$\boldsymbol{\beta} = \sum_{i=1}^{3} \beta_i \hat{d}_i \tag{10}$$

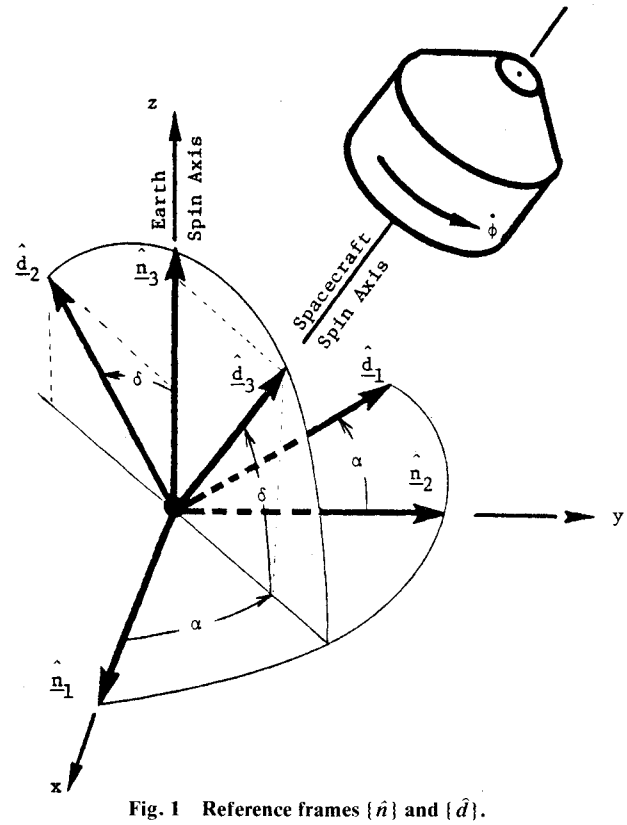

Fig. 1 Reference frames $\{\hat{n}\}$ and $\{\hat{d}\}$.

is the geomagnetic field vector with $\{\hat{d}\}$ components

$$\begin{Bmatrix} \beta_1 \\ \beta_2 \\ \beta_3 \end{Bmatrix} = \begin{bmatrix} -\sin\alpha & \cos\alpha & 0 \\ -\sin\delta\cos\alpha & -\sin\delta\sin\alpha & \cos\delta \\ \cos\delta\cos\alpha & \cos\delta\sin\alpha & \sin\delta \end{bmatrix} [R(\theta(t),\Phi(t),\lambda(t))] \begin{Bmatrix} B_1 \\ B_2 \\ B_3 \end{Bmatrix} \tag{11a}$$

$$[R(\theta,\Phi,\lambda)] = \begin{bmatrix} \cos\theta & -\sin\theta & 0 \\ \sin\theta & \cos\theta & 0 \\ 0 & 0 & 1 \end{bmatrix} \begin{bmatrix} -\sin\Phi\cos\lambda & -\sin\lambda & -\cos\Phi\cos\lambda \\ -\sin\Phi\sin\lambda & \cos\lambda & -\cos\Phi\sin\lambda \\ \cos\Phi & 0 & -\sin\Phi \end{bmatrix} \tag{11b}$$

projects geomagnetic Earth-fixed components of the magnetic field into Earth-centered, nonrotating rectangular components

$$\begin{Bmatrix} B_1 \\ B_2 \\ B_3 \end{Bmatrix} = \sum_{n=1}^{N} \frac{1}{r^{n+2}} \begin{Bmatrix} \displaystyle\sum_{m=0}^{n} \frac{dP_n^m(\sin\Phi)}{d\Phi} [G_n^m \cos m\lambda + H_n^m \sin m\lambda] \\ \dfrac{1}{\cos\Phi} \displaystyle\sum_{m=1}^{n} mP_n^m(\sin\Phi) [G_n^m \sin m\lambda - H_n^m \cos m\lambda] \\ -(n+1) \displaystyle\sum_{m=0}^{n} P_n^m(\sin\Phi) [G_n^m \cos m\lambda + H_n^m \sin m\lambda] \end{Bmatrix} \tag{12}$$

where G_n^m, H_n^m are harmonic coefficients,[14] $P_n^m(\sin\Phi)$ are associated Legendre functions, and $\{B_1,B_2,B_3\}^T$ is the geomagnetic field vector (down, east, north),

$$\begin{Bmatrix} x_e \\ y_e \\ z_e \end{Bmatrix} = \begin{bmatrix} \cos\theta & \sin\theta & 0 \\ -\sin\theta & \cos\theta & 0 \\ 0 & 0 & 1 \end{bmatrix} \begin{Bmatrix} x \\ y \\ z \end{Bmatrix} \tag{13}$$

rectangular, equatorial, Earth-fixed position of the spacecraft, $\{x,y,z\}^T$ is the instantaneous spacecraft rectangular position (from an orbit integration) in a recent equatorial nonrotating coordinate system,

$$\begin{aligned} r &= [x^2+y^2+z^2]^{1/2} && \text{radial distance to satellite} \\ \lambda &= \tan^{-1}(x_e/y_e) && \text{geographic east longitude} \\ \Phi &= \sin^{-1}(z/r) && \text{geographic north latitude} \end{aligned} \tag{14}$$

Thus, from Eqs. (11), the $\{\hat{d}\}$ components of the geomagnetic field have the functional dependence

$$\beta_i = \text{function}_i(\alpha,\delta,t) \qquad (i=1,2,3) \tag{15}$$

for specified initial conditions on the orbital motion.

Upon carrying out the substitution of Eqs. (9) and (10) into Eq. (8), one obtains

$$T_1 = -pM\beta_2 = \text{function}(\alpha,\delta,p,t)$$

$$T_2 = pM\beta_1 = \text{function}(\alpha,\delta,p,t) \qquad T_3 = 0 \tag{16}$$

and substituting Eqs. (16) into Eqs. (7), slow maneuvers are governed by the pair of equations

$$\dot{\alpha} = pf_1(\alpha,\delta,t) \qquad \dot{\delta} = pf_2(\alpha,\delta,t) \tag{17}$$

where

$$f_1 = -m\beta_2/\cos\delta \qquad f_2 = m\beta_1 \qquad m = M/H_3 = \text{const}$$

Optimal Control Formulation

We seek to minimize maneuver time $= \int_{t_0}^{t_f} dt$ subject to the requirement that the terminal states are specified

$$\alpha(t_0) = \alpha_0 \qquad \delta(t_0) = \delta_0 \tag{18a}$$

$$\alpha(t_f) = \alpha_f \qquad \delta(t_f) = \delta_f \tag{18b}$$

and the trajectory is given by the solution of Eqs. (17) with the control variable constraint that the polarity satisfies

$$|p(t)| \le 1 \tag{19}$$

Preparing to apply Pontryagin's Principle,[13] we introduce the Hamiltonian functional

$$\mathcal{H} = 1 + p(\lambda_1 f_1 + \lambda_2 f_2) \tag{20}$$

where λ_1 and λ_2 are costate variables. Pontryagin's necessary conditions require, in addition to Eqs. (17-19) that the costate variables satisfy the adjoint system to differential equations

$$\dot{\lambda}_1 = -\frac{\partial \mathcal{H}}{\partial \alpha} = -p\left[\frac{\partial f_1}{\partial \alpha}\lambda_1 + \frac{\partial f_2}{\partial \alpha}\lambda_2\right]$$

$$\dot{\lambda}_2 = -\frac{\partial \mathcal{H}}{\partial \delta} = -p\left[\frac{\partial f_1}{\partial \delta}\lambda_1 + \frac{\partial f_2}{\partial \delta}\lambda_2\right] \tag{21}$$

and the control polarity $p(t)$ is determined to minimize $\mathcal{H}(p(t))$ from Eq. (20), yielding the "polarity switching function"

$$p(t) = -\text{sign}[\lambda_1 f_1 + \lambda_2 f_2] \tag{22}$$

It is evident, since Eqs. (21) and (22) contain the λ's linearly, and they do not appear explicitly elsewhere, that a linear scaling of λ's by a positive constant is immaterial; in other words, the λ's do not have a unique magnitude.

We are, therefore, free to arbitrarily constrain the λ's magnitude; we adopt the constraint that the initial costates lie on the unit circle

$$\lambda_1^2(t_0) + \lambda_2^2(t_0) = 1$$

Strictly speaking, this condition is inconsistent with the transversality condition $\mathcal{H}(t) = 0$ typically imposed[13] for control problems having free final time. However, since extremizing $C\int_{t_0}^{t_f} dt$ is equivalent to extremizing $\int_{t_0}^{t_f} dt$ for C, an unspecified positive constant, then a Hamiltonian $\mathcal{H} = C + p(\lambda_1 f_1 + \lambda_2 f_2)$ can be introduced with exactly the same resulting costate equations, Eqs. (21), and switching function, Eq. (22). Since an infinity of C values can be chosen, the $\lambda_1^2(t_0) + \lambda_2^2(t_0) = 1$ condition is legal since it merely chooses implicitly one of these possible normalizations. If desired, the value of C is simply determined as $[-p(\lambda_1 f_1 + \lambda_2 f_2)]_{t_f}$.

Accordingly, we restrict the initial costates to lie on the unit circle and introduce an initial phase angle γ_0 such that

$$\lambda_1(t_0) = \cos\gamma_0 \qquad \lambda_2(t_0) = \sin\gamma_0 \qquad (0 \le \gamma_0 < 360 \text{ deg}) \tag{23}$$

Sweeping γ_0 from 0-360 deg determines a complete family of initial costates. Each costate pair generates a minimum time trajectory $[\alpha(t),\delta(t)]$ from integration of Eqs. (17) and (21) with initial conditions, Eqs. (18a) and (23); the optimum polarity switches being given by Eq. (22). For each trial value on the initial costate phase γ_{0i}, it is necessary to search for the time of closest approach [wherein $\alpha(t)_i$, $\delta(t)_i$ most nearly coincides with the desired α_f,δ_f]; each γ_{0i} which generates a time-optimal trajectory passing within, for example, 0.5 deg of (α_f,δ_f), is a candidate local extremal. Due to small amplitude time-varying geomagnetic harmonics and the present state of knowledge of the static geomagnetic field, we believe it is not realistic to discuss magnetic control for tolerances much less than 0.5 deg. Through the use of interactive graphics, optimal solutions can be routinely determined in 15 min of real time. As will be evident, the minimum time maneuver is not always unique, but the ease with which the extremal field map can be generated and displayed allows confident selection of the global minimum time maneuver.

For convenient reference, the minimum time-optimal maneuver necessary conditions are collected below in back substitution form, including the partial derivatives required in Eqs. (21):

$$\dot{\alpha} = pf_1(t,\alpha,\delta) \qquad \dot{\delta} = pf_2(t,\alpha,\delta)$$

$$\dot{\lambda}_1 = -p\left[\frac{\partial f_1}{\partial \alpha}\lambda_1 + \frac{\partial f_2}{\partial \alpha}\lambda_2\right] \qquad \dot{\lambda}_2 = -p\left[\frac{\partial f_1}{\partial \delta}\lambda_1 + \frac{\partial f_2}{\partial \delta}\lambda_2\right] \tag{24}$$

$$p(t) = -\text{sign}[\lambda_1 f_1 + \lambda_2 f_2]$$

where

$$f_1 = -m\beta_2/\cos\delta \quad f_2 = m\beta_1 \quad m = M/H_3 \qquad H_3 = C\dot{\phi} = \text{const}$$

$$\frac{\partial f_1}{\partial \alpha} = -m\frac{\partial \beta_2}{\partial \alpha}\left(\frac{1}{\cos\delta}\right) \quad \frac{\partial f_1}{\partial \delta} = -m\left(\frac{\partial \beta_2}{\partial \delta} - \beta_2\tan\delta\right)\left(\frac{1}{\cos\delta}\right)$$

$$\frac{\partial f_2}{\partial \alpha} = m\frac{\partial \beta_1}{\partial \alpha} \qquad \frac{\partial f_2}{\partial \delta} = m\frac{\partial \beta_1}{\partial \delta} \tag{25a}$$

where $\{\beta_1,\beta_2,\beta_3\}$ is the geomagnetic field vector with $\{\hat{d}\}$ components, a function of $\{r(t), \lambda(t), \Phi(t), \alpha, \delta, B_1, B_2, B_3\}$, as in Eqs. (11), $\{B_1, B_2, B_3\}$ is the geomagnetic field vector with down, east, north components, computed via a user-prescribed model as a function of $\{\Phi(t), \lambda(t), r(t)\}$, for example, Eq. (12).

$$\Phi(t) = \sin^{-1}(z(t)/r(t)) \qquad \lambda(t) = \tan^{-1}(y_e(t)/x_e(t))$$

$$r(t) = [x^2(t) + y^2(t) + z^2(t)]^{1/2} \tag{25b}$$

$$\begin{Bmatrix} x_e(t) \\ Y_e(t) \\ z_e(t) \end{Bmatrix} = \begin{bmatrix} \cos\theta(t) & \sin\theta(t) & 0 \\ -\sin\theta(t) & \cos\theta(t) & 0 \\ 0 & 0 & 1 \end{bmatrix} \begin{Bmatrix} x(t) \\ y(t) \\ z(t) \end{Bmatrix} \quad (25c)$$

= Earth-fixed rectangular (equatorial) coordiantes of the satellite

and where $\{x(t),y(t),z(t)\}$ are satellite rectangular coordinates (nonrotating, equatorial) from user-prescribed orbital equations of motion,

$$\theta(t) = \theta_{\text{ref}} + \omega_e(t - t_{\text{ref}}) = \text{sideral time of Greenwich} \quad (25d)$$

where ω_e is the sideral angular rate of Earth's rotation, and θ_{ref} is the sideral angle of Greenwich at time t_{ref}

$$\frac{\partial}{\partial\alpha}\begin{Bmatrix} \beta_1 \\ \beta_2 \\ \beta_3 \end{Bmatrix} = \begin{bmatrix} -\cos\alpha & -\sin\alpha & 0 \\ \sin\delta\sin\alpha & -\sin\delta\cos\alpha & 0 \\ -\cos\delta\sin\alpha & \cos\delta\cos\alpha & 0 \end{bmatrix} [R(\theta,\Phi,\lambda)] \begin{Bmatrix} B_1 \\ B_2 \\ B_3 \end{Bmatrix} \quad (25e)$$

$$\frac{\partial}{\partial\delta}\begin{Bmatrix} \beta_1 \\ \beta_2 \\ \beta_3 \end{Bmatrix} = \begin{bmatrix} 0 & 0 & 0 \\ -\cos\delta\cos\alpha & -\cos\delta\sin\alpha & -\sin\delta \\ -\sin\delta\cos\alpha & -\sin\delta\sin\alpha & \cos\delta \end{bmatrix} [R(\theta,\Phi,\lambda)] \begin{Bmatrix} B_1 \\ B_2 \\ B_3 \end{Bmatrix} \quad (25f)$$

and $[R(\theta(t), \Phi(t), \lambda(t))] =$ Eq. (11b).

Example Calculations of Optimal Maneuvers

In solution of the two-point boundary-value problems, it is convenient to use a modified inertial reference frame. This modified inertial frame $\{\hat{n}^*\}$ is constructed as follows:

$$\hat{n}_1^* = \hat{l}_f = (\cos\delta_f\cos\alpha_f)\hat{n}_1 + (\cos\delta_f\sin\alpha_f)\hat{n}_2 + (\sin\delta_f)\hat{n}_3$$

$$\hat{l}_0 = (\cos\delta_0\cos\delta_0)\hat{n}_1 + (\cos\delta_0\sin\alpha_0)\hat{n}_2 + (\sin\delta_0)\hat{n}_3$$

$$\hat{n}_2^* = \hat{n}_3^* \times \hat{n}_1^* \qquad \hat{n}_3^* = \hat{l}_f \times \hat{l}_0 / |\hat{l}_f \times \hat{l}_0| \quad (26)$$

Equations (26) can be collected as

$$\{\hat{n}^*\} = [C]\{\hat{n}\} \quad (27)$$

where $[C]$ is the resulting constant direction cosine matrix. The optimal control formulation remains valid for this special inertial frame; it is necessary to (everywhere above) replace $[R]$ of Eq. (11b) by

$$[R^*] = [R][C^T] \quad (28)$$

In the event of 180 deg maneuvers, we take (in lieu of the last of Eqs. (26))

$$\hat{n}_3^* = \hat{l}_f \times \hat{n}_3$$

To avoid ambiguity, we use (α^*,δ^*) to denote the angles analogous to (α,δ) defined with respect to $\{\hat{n}^*\}$. Note the desired consequence that $[\alpha^*(t_0), \delta^*(t_0)]$ and $[\alpha^*(t_f),\delta^*(t_f)]$ locate points on the "equator" of the $\{\hat{n}^*\}$ system, and the final state $[\alpha^*(t_f),\delta^*(t_f)]$ lies at either the origin (0,0) or $(2\pi,0)$; these properties simplify and universalize methods for solving the TPBVP.

To illustrate the determination of optimal maneuvers using the methods of this paper, we adopt the NOVA vehicle and orbit parameters in Table 1. The objective is to find the sequence of switching times to maneuver from the initial state ($\alpha_0 = 45.2$ deg, $\delta_0 = 35.1$ deg) to the desired final state ($\alpha_f = -45.0$ deg, $\delta_f = -30.0$ deg).

Figure 2 displays an extremal field of trajectories (relative to $\{\hat{n}^*\}$) generated by sweeping γ_0 from 0 to 360 deg at an increment of 60 deg; this rather large step was taken to allow an interactive graphics user to immediately note that the trajectory to the origin appears to be contained in the interval ($0 < \gamma_0 < 60$ deg), and that the trajectory to the point $X(2\pi,0)$ appears to be contained in the interval ($180 < \gamma_0 < 360$ deg). Subsequent exploration (Fig. 3) for the optimal solution A to the origin reveals $\gamma_0 \cong 30$ deg generates the desired extremal. Extremal A required 7.20 h and 19 polarity switches (Table 2) to complete the maneuver. The results of Table 2 were generated by integrating Eqs. (4) and reflect about 2 deg accumulated errors from the approximations implicit in Eqs. (6).

The search for the second solution in the interval ($180 < \gamma_0 < 360$ deg) is more laborious, but two intermediate trials led to the family of trajectories displayed in Fig. 4; it is evident that the solution lies in the interval ($335 < \gamma_0 < 340$ deg). One subsequent iteration (Fig. 5) reveals that $\gamma_0 = 336$ deg generates extremal B; this solution required 15.50 h and 41 polarity switches (Table 3). The longer maneuver time of 15.5 h did not result in a large error accumulation (≈ 3 deg). It is anticipated that a restart will be done after typically 10 h of maneuver time to minimize the impact of these errors. It is clearly preferable to execute the more intuitively appealing maneuver A. Intuition will prove less reliable for maneuvers near 180 deg, mainly due to Earth rotation and orbital eccentricity effects, in addition to asymmetries in the geomagnetic field.

The (α,δ) history of maneuvers A and B are displayed in Fig. 6. The fine structure of Figs. 3 and 5 are not in evidence since the curves of Fig. 6 are simply straight-line connection of the states at polarity switch times.

The entire sequence of displays and calculations (summarized in Figs. 2-6 and Tables 1-3) were generated in less than 15 min of real time. It has been found much more attractive to display successive trajectory families on an in-

Table 1 Typical NOVA parameters

t_0 = year 1980, day 320, hour 12, min 0 (GMT)
M = 69,600 pole-cm = 69.600 amp-m^2
$\dot{\phi}$ = 5 rpm
I_3 = 34 kg-m^2
a = orbit semimajor axis = 1.102818 Earth radii
e = eccentricity = 0.029192
i = inclination = 89.290 deg
ω = arg. of perigee = 24.870 deg
Ω = arg. of ascending node = 336.602 deg
$di/dt = 0$
$d\omega/dt = -3.536$ deg/day
$d\Omega/dt = -0.0876$ deg/day

Table 2 Optimal maneuver A

Command no.	Day	Hour	Minute	$p(t)$	$\alpha(t)$	$\delta(t)$
1	320	12	0	−1	45.2	35.1
2	320	12	17	1	39.7	29.7
3	320	12	45	−1	44.2	22.4
4	320	13	9	1	40.8	17.9
5	320	13	32	−1	42.9	10.5
6	320	13	57	1	36.5	4.1
7	320	14	23	−1	37.6	−2.8
8	320	14	49	1	31.0	−6.1
9	320	15	11	−1	30.8	−12.4
10	320	15	37	1	21.8	−17.2
11	320	16	1	−1	20.1	−22.6
12	320	16	28	1	9.8	−23.7
13	320	16	50	−1	7.0	−27.9
14	320	17	17	1	−4.7	−29.9
15	320	17	39	−1	−9.1	−32.7
16	320	18	8	1	−21.5	−31.0
17	320	18	30	−1	−26.0	−32.8
18	320	18	57	1	−38.3	−32.0
19	320	19	12	0	−42.7	−31.4

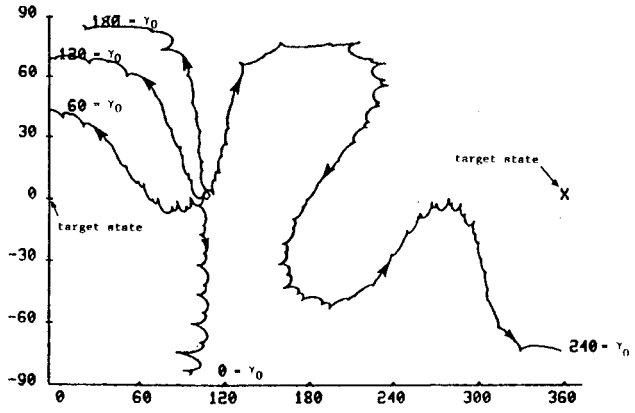

Fig. 2 Minimal time extremal field map.

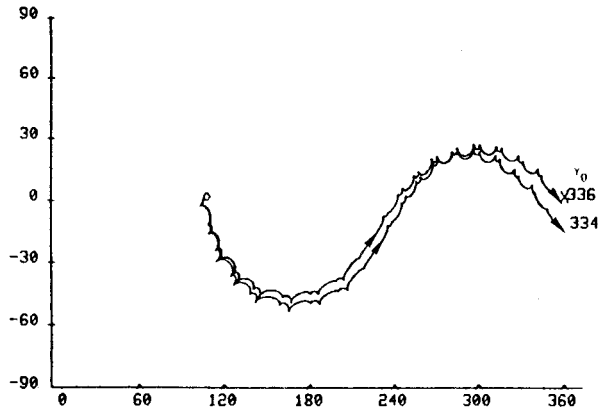

Fig. 5 Converged maneuver B.

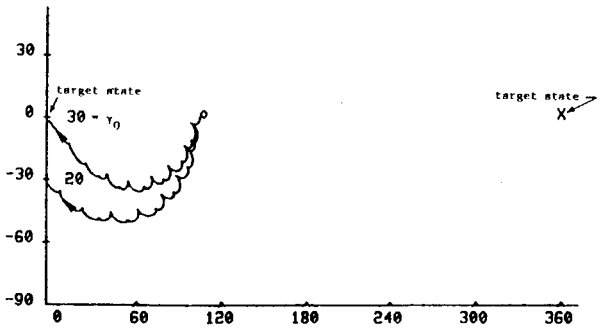

Fig. 3 Converged maneuver A.

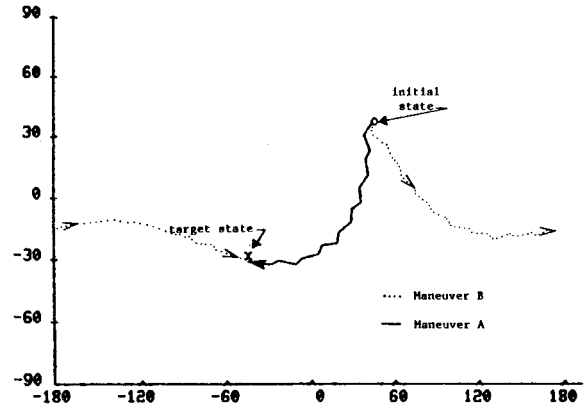

Fig. 6 Converged (α,δ) trajectories for maneuvers A and B.

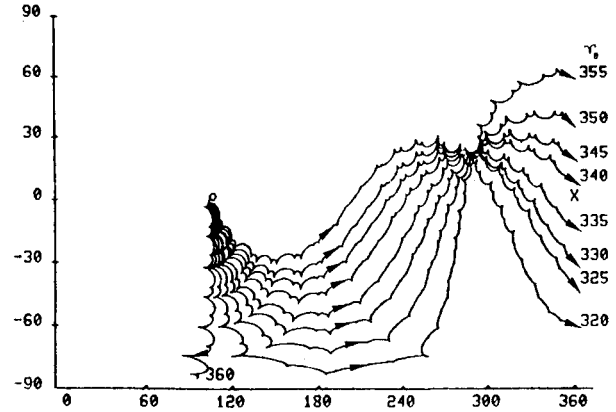

Fig. 4 Extremal field trajectories near $\gamma_0 = 335$ deg.

teractive CRT, rather than constructing elaborate logic to automate solution of the TPBVP. The possibility of singular sub-arcs [along which the switch function, Eq. (22), identically vanishes] is a mathematical possibility. The existence of these cases was not dealt with in this work, although we did some numerical searches which suggest that they do not exist, for practical values of magnet pole strength. The maneuvers are not generally unique, in the sense that at least two maneuvers between the same terminal points generally exist. Except with ±10 deg of the 180 deg transfer case, one can usually discard the solution requiring greater than 180 deg slewing since it will almost always require more time.

Table 3 Optimal maneuver B

Command no.	Day	Hour	Minute	$p(t)$	$\alpha(t)$	$\delta(t)$
1	320	12	0	−1	45.2	35.1
2	320	12	9	1	44.3	31.0
3	320	12	39	−1	54.4	25.1
4	320	13	1	1	56.4	21.2
5	320	13	27	−1	63.7	15.1
6	320	13	46	1	65.6	10.1
7	320	14	15	−1	75.3	4.9
8	320	14	37	1	77.2	0.8
9	320	15	4	−1	85.7	−3.2
10	320	15	23	1	88.2	−7.1
11	320	15	51	−1	99.0	−10.2
12	320	16	12	1	101.7	−14.2
13	320	16	40	−1	112.2	−14.7
14	320	16	59	1	115.6	−17.0
15	320	17	27	−1	127.3	−17.5
16	320	17	48	1	131.3	−20.2
17	320	18	17	−1	142.3	−17.6
18	320	18	36	1	146.1	−19.0
19	320	19	3	−1	157.6	−17.5
20	320	19	24	1	162.3	−18.1
21	320	19	52	−1	172.8	−15.2
22	320	20	12	1	176.6	−15.8
23	320	20	40	−1	−172.2	−13.5
24	320	21	0	1	−167.8	−12.7
25	320	21	28	−1	−157.5	−12.0
26	320	21	48	1	−153.8	−12.0
27	320	22	17	−1	−142.6	−10.9
28	320	22	36	1	−138.4	−10.6
29	320	23	5	−1	−128.0	−12.1
30	329	23	24	1	−124.3	−11.7
31	320	23	54	−1	−113.0	−12.9
32	321	0	13	1	−109.2	−14.0
33	321	0	42	−1	−98.5	−16.1
34	321	1	1	1	−95.0	−16.8
35	321	1	30	−1	−83.5	−19.9
36	321	1	50	1	−79.7	−21.9
37	321	2	20	−1	−68.2	−22.9
38	321	2	38	1	−64.7	−25.1
39	321	3	7	−1	−52.2	−28.0
40	321	3	27	1	−48.0	−29.6
41	321	3	30	0	−47.8	−29.8

Concluding Remarks

We provide a formulation for time-optimal magnetic maneuvers for spin-stabilized symmetric spacecraft. Simulations support the conclusion that the method is convenient and practical for rapidly determining these maneuvers in a near-real-time satellite control environment. The departure of the vehicle from the idealizations herein, and the failure to perfectly realize the commanded control will result in gradual divergence of the actual motion from the optimal maneuver. For this reason, each mission should be preceded by simulations designed to generate conservative guidelines on the time interval over which the approach can be employed without restarting.

Acknowledgments

This work was carried out primarily at The Johns Hopkins Applied Physics Laboratory; the support and suggestions of H.D. Black are gratefully acknowledged. In parallel studies carried out at VPI&SU, the work of William Baracat was especially noteworthy. The comments of D. Sonnabend and K.T. Alfriend are also appreciated.

References

[1] Tossman, B.E., "A Time Optimal Geomagnetic Maneuvering Technique for Orbit Correction Thrust Vectoring," *Proceedings of the 12th International Symposium on Space Technology and Science* (Tokyo, 1977), Pergamon Press, New York, 1977, pp. 389-398.

[2] Tossman, B.E., "Magnetic Attitude Control System for the Radio Astronomy Explorer-A Satellite," *Journal of Spacecraft and Rockets,* Vol. 6, March 1969, pp. 239-244.

[3] Shiegehara, M., "Geomagnetic Attitude Control of an Axisymmetric Spinning Satellite," *Journal of Spacecraft and Rockets,* Vol. 9, June 1972, pp. 391-398.

[4] Kershner, R.B. and Newton, R.R., "The TRANSIT System," *Journal of the Institute of Navigation,* Vol. 15, 1962, pp. 129-144.

[5] Grasshoff, L.H., "A Method for Controlling the Attitude of a Spin-Stabilized Satellite," *ARS Journal,* Vol. 31, May 1961, pp. 646-649.

[6] Renard, M.L., "Command Laws for Magnetic Attitude Control of Spin-Stabilized Earth Satellites," *Journal of Spacecraft and Rockets,* Vol. 4, Feb. 1967, pp. 156-163.

[7] Sorensen, J.A., "A Magnetic Attitude Control System for an Axisymmetric Spinning Spacecraft," *Journal of Spacecraft and Rockets,* Vol. 8, May 1971, pp. 441-448.

[8] Rajaram, S. and Goel, P.S., "Magnetic Attitude Control of Near Earth Spinning Satellites," *Journal of the British Interplanetary Society,* Vol. 31, 1978, pp. 163-167.

[9] Goel, P.S. and Rajaram, S., "Magnetic Attitude Control of a Momentum-Biased Satellite in Near-Equatorial Orbit," *Journal of Guidance and Control,* Vol. 2, July-Aug. 1979, pp. 334-338.

[10] Alfriend, K.T., "Magnetic Attitude Control System for Dual-Spin Satellites," *AIAA Journal,* Vol. 13, June 1975, pp. 817-822.

[11] Stickler, A.C. and Alfriend, K.T., "Elementary Magnetic Attitude Control System," *Journal of Spacecraft and Rockets,* Vol. 13, May 1976, pp. 282-287.

[12] Takezawa, S. and Ninomiya, K., "A New Approach to the Analysis and Design of Magnetic Stabilization of Satellites," *Proceedings of the 30th Congress of the IAF,* Paper IAF-79-106, Pergamon Press, New York, Sept. 1979.

[13] Kirk, D.C., *Optimal Control Theory,* Prentice-Hall, Englewood Cliffs, N.J., 1971.

[14] Strumanis, M., "Geomagnetic Field Model," an IBM 360 Library Program Documentation of BMAG, The Johns Hopkins Applied Physics Lab., Laurel, Md., Dec. 1968.